Frond-level analyses reveal functional heterogeneity within heavy metal-treated duckweed colonies

Viktor Oláh [a,*], Kamilla Kosztankó [a], Muhammad Irfan [a], Zsuzsanna Barnáné Szabó [a],
Marcel A. K Jansen [b], Sándor Szabó [c], Ilona Mészáros [a]

[a] Department of Botany, Institute of Biology and Ecology Faculty of Science and Technology, University of Debrecen, Egyetem square 1, Debrecen, Hungary, Zip, Debrecen H-4032, Hungary
[b] School of Biological, Earth and Environmental Science, University College Cork, Distillery Fields, North Mall, Cork T23N73K, Ireland
[c] Department of Biology, University of Nyiregyhaza, Nyiregyhaza H-4401, Hungary

A R T I C L E I N F O

A B S T R A C T

Duckweeds (*Lemnaceae*) rapidly produce clonal populations that make them ideal models in plant physiological and ecotoxicological research. Yet, despite their genetic homogeneity, duckweed colonies are clusters of successively produced fronds with different ontogenetic states, and this heterogeneity has rarely been studied. We analyzed frond-level photosynthetic responses of three duckweed species (*Spirodela polyrhiza, Landoltia punctata* and *Lemna minor*) to hexavalent chromium and nickel by means of chlorophyll fluorescence imaging. Our aim was to test whether fronds, or frond zones in their different developmental stages respond differently to heavy metal stress. Different response patterns were found for the three tested species. Young fronds of *S. polyrhiza* were more sensitive to chromate but less affected by nickel compared to mature ones, while in *La. punctata* the opposite was found. In *Le. minor* cultures, young fronds were more sensitive to both heavy metals compared to mature ones. Within-frond patterns indicated that chromate inhibited the marginal frond regions strongest. In *La. punctata* and *Le. minor*, nickel was most detrimental in the developing frond regions. In contrast, in *S. polyrhiza* the middle zone of both young and mature fronds was affected strongest by nickel. The observed patterns suggest that internal redistribution of toxicants plays a key role in shaping duckweed responses.

Results highlight that ontogenetically different parts of duckweed plants respond differently to environmental stimuli. Since duckweed-based impact studies and economical applications rely strongly on the interactions between the duckweed colony and its environment, frond-, and within-frond level analysis of duckweed responses comprise a unique tool to reveal uptake, re-distribution and mode of action of environmentally relevant substances.

1. Introduction

Duckweeds (*Lemnaceae*) form a monophyletic group of free-floating freshwater plants that have undergone a significant evolutionary reduction (Tippery et al., 2021). Their thallus-like body –the frond– basically consists of an upper and lower epidermis and an assimilating, aerenchymatous mesophyll with meristematic regions ("pockets" or "pouches") in the basal part. Depending on the degree of reduction, the fronds may also contain vascular elements ("veins") and adventitious roots, both originating at the node of the frond.

The morphological and anatomical reduction of *Lemnaceae* fronds is paralleled by functional changes. One of these changes is that duckweeds absorb nutrients directly through their weakly cutinized abaxial (lower) epidermis. Roots may also contribute to nutrient uptake (Cedergreen and Madsen, 2002), but experimental evidence indicates that they are dispensable (Ware et al., 2023). Whether epidermal nutrient uptake is uniform over the entire abaxial frond surface, or whether the uptake is rather localized in "hotspots", is not yet clear. A previous study suggested that heavy metal uptake was not uniform, but rather that node-zone and the roots displayed the highest uptake rate of cadmium (Xu et al., 2018). The functional significance of veins in fronds is similarly enigmatic. They play role in distributing nutrients and assimilates throughout the frond. However, the small frond size, thin mesophyll, and epidermal nutrient uptake may also allow adequate

---

* Corresponding author.
  E-mail address: olahviktor@unideb.hu (V. Oláh).

internal distribution via direct intercellular transport. The phylogenetically youngest Wolffioideae genera lack roots and contain only remnants of vascular tissue (Landolt, 1986). To our knowledge, however, there is no decisive evidence on the actual contribution of veins to within-frond distribution of nutrients and assimilates. Analyses of nickel- and chromate treated duckweeds using X-ray fluorescence (µXRF) technology revealed uneven distribution of the metals within the fronds, and this can be due to either uneven uptake or uneven distribution (Oláh et al., 2023). Consequently, there is a need to further clarify the acquisition, transport, and storage of nutrients and toxicants within duckweed fronds (Abramson et al., 2022).

In the context of environmental responses, the peculiar way of producing offspring in duckweeds needs to be considered too. Descendants are formed by the meristem of mature fronds, and this occurs within a pouch contained within the mother frond. Once formed, duckweed fronds develop and mature basipetally, that is distal (apical) frond segments reach their final size and anatomy earlier than the basal (proximal) parts (Lemon and Posluszny, 2000). Different frond generations usually stay connected in larger clusters (colonies). This structure allows exchange of nutrients and assimilates between fronds (Demmig-Adams et al., 2022), but the cohabitation is not guaranteed. In fact, a common duckweed response to acute stress is breaking up colonies into smaller clusters or single fronds, presumably to increase the survival chances for at least some fronds (Henke et al., 2011; Peršić et al., 2022).

It can be hypothesized that different ontogenetic stages will differentially modulate uptake, transport, and biological impacts of pollutants. Yet, the duckweed literature mostly reports averaged (across colonies) responses of species to environmental factors. Imaging-based phenotyping methods may offer a means to tell apart responses of individual fronds or even different parts of the same frond. Zinc and paraquat sensitivities, as examples, proved to be the function of frond age (Lahive et al., 2012; Park et al., 2020).

Duckweeds are extensively used in plant physiology and ecotoxicology research as higher plant models (OECD, 2006; Acosta et al., 2021). In addition, their economic potential as water remediating agents and novel crops gains significance as well (Paolacci et al., 2022; Petersen et al., 2022; Szabó et al., 2023). All the above applications rely strongly on the interactions between duckweed colonies and their environment, including uptake and re-distribution of nutrients and/or toxins within and between fronds.

The aim of this study was to assess duckweed responses to heavy metals at the level of individual fronds and within-frond segments. Three duckweed species, namely *S. polyrhiza, Landoltia punctata* and *Lemna minor*, were treated with nickel and hexavalent chromium, and photosynthetic responses were analyzed using *in vivo* chlorophyll fluorescence imaging. This method has proved its suitability in studying duckweed responses to various agents (Oláh et al., 2021), and also enables morphometric analyses (Pietrini et al., 2019).

The specific questions we studied in the present paper were as follows:

(i) is there a functional difference in the metal-induced responses of fronds at different ontogenetic stages and in different parts of fronds?

(ii) are the response patterns consistent among the species and heavy metals?

2. Materials and methods

2.1. Stock culturing and experimental design

Axenic laboratory cultures of the three duckweed species, *Spirodela polyrhiza* (L.) Schleid. clone UD0401 (lake Kis-Balaton, W. Hungary, Oláh et al., 2018), *Landoltia punctata* (G. Meyer) Les & Crawford clone #7760 (Landolt clone, S. Australia) and *Lemna minor* L. clone UD0201 (E. Hungary, Oláh et al., 2010) were used. The stock cultures were maintained in 300 ml Erlenmeyer flasks, in Steinberg's medium (pH 6.0 ± 0.2, Environment Canada, 2007), under constant temperature (24±2

°C) and irradiation (PPFD 60±10 µE m^{-2} s^{-1}, white light, Oláh et al., 2021).

Healthy colonies from 7 to 8 days-old stock cultures were used for the experimental work. The heavy metal treatments were conducted in 12-well tissue culturing plates, containing 4 ml of either pure Steinberg's medium (control), or the same medium with 4 mg l^{-1} Cr(VI) (applied as K$_2$Cr$_2$O$_7$), or 2.5 mg l^{-1} Ni (applied as NiSO$_4$ x 7 H$_2$O) in each well, respectively. The experimental setup and the applied heavy metal concentrations were adapted from previous works with the same clones (Oláh et al., 2021, 2023), and aimed at inducing considerable impact on plant growth and photosystem II (PSII) photochemistry but not triggering frond mortality by the end of the treatment duration. The starting inoculum was 1 colony per well, corresponding to 3.3 ± 0.7 fronds for *S. polyrhiza*; 3.8 ± 1.6 fronds for *La. punctata* and 3.3 ± 0.5 fronds for *Le. minor*, respectively. The heavy metal exposures lasted for 72±2 h under identical ambient conditions as for stock culturing. For preparing the Steinberg's medium and heavy metal treatments, reagent grade chemicals and Type I. ultrapure water were used.

The tests in multi-well plates were conducted with 4 parallel wells for each treatment, and the experiments were repeated three times with *S. polyrhiza* and *La. punctata* (resulting in a total of $n = 12$ wells per treatment), and two times with *Le. minor*, resulting in a total of $n = 8$ wells per treatment for this species.

2.2. In vivo chlorophyll fluorescence measurements

On the starting (0 d) and finishing (3 d) days of the experiments, dark adapted *in vivo* chlorophyll fluorescence induction parameters of the test plants' photosystem II (PSII) were assessed by means of an ImagingPam M-series chlorophyll fluorometer (Walz GmbH, Effeltrich, Germany), using a previously reported protocol (Oláh et al., 2021). In short, following a 30 min-long dark adaption, the base fluorescence (Fo) and maximal fluorescence (Fm) of plants were determined using weak, non-inducible measuring light flashes (~100 ms pulses at 1 Hz frequency), and a strong light pulse (~4000 µE m^{-2} s^{-1}) for 720 ms. After recording Fo and Fm, a moderate (~77 µE m^{-2} s^{-1}) actinic illumination was applied for 10 min to reach steady-state photosynthesis. At the end of this period, steady-state fluorescence (Fs) and, by applying a second saturating light pulse, light-acclimated maximal fluorescence (Fm') were determined.

We used the built-in LED light source (blue, 450 nm) of the instrument to measure modulated fluorescence, as well as to generate saturating light pulses and continuous actinic illumination. Based on the Fo, Fm, Fs and Fm' values measured on the 3rd day of treatments, further indices were derived pixel-by-pixel by means of the ImagingWinGigE software (Walz GmbH, Germany) as follows:

Fv/Fm = (Fm-Fo)/Fm = maximum (or potential) quantum yield of PSII photochemistry (Roháček, 2002)

Y(II) = (Fm'-Fs)/Fm' = effective (or actual) quantum yield of photochemical energy conversion in PSII under the applied light intensity and ambient conditions (Roháček, 2002)

Y(NPQ) = (Fs/Fm')-(Fs/Fm) = quantum yield of regulated non-photochemical energy dissipation in PS II (Klughammer and Schreiber, 2008)

Y(NO) = Fs/Fm = quantum yield of non-regulated heat dissipation and fluorescence emission (Klughammer and Schreiber, 2008)

Fv/Fm, Y(II), Y(NPQ) and Y(NO) were averaged on a well basis and were used to characterize the overall photosynthetic performance of cultures.

The instrument allowed simultaneous measurements of all plants in a 12-well plate, and imaged chlorophyll fluorescence signals at a 1392×1040 pixel (~1,5 Mpixel) nominal resolution. As the instrument automatically bins the neighboring 2 × 2 pixels, the final resolution of the obtained images was 640×480 pixels, which resulted in ~0.22 mm (4.6 pixel mm^{-1}) spatial resolution in the applied experimental setup.

2.3. Image analysis

Chlorophyll fluorescence images of the plates allowed extraction of different types of information. For example, using the Fv/Fm-images of the plates, taken on the 0th and 3rd days of the treatments, we counted fronds in each well. Then we calculated the frond number-based relative growth rate (RGR$_{FN}$) as a general proxy of plant fitness (OECD, 2006):

$$RGR_{FN} \; (day^{-1}) = (lnFN_3 - lnFN_0)/3$$

where FN$_0$ and FN$_3$ are the respective frond numbers at the 0th and 3rd days, and 3 is the exposure time in days.

Additionally, on the 3rd day of treatments we also counted the number of colonies and then determined the colony size as follows:

$$colony \; size = N_{frond}/N_{colony}$$

where N$_{frond}$ is the total number of fronds and N$_{colony}$ is the number of colonies in the respective well.

In order to obtain frond-level data, we exported the chlorophyll fluorescence images of plates taken on the 3rd day by the ImaginWinGigE software as 256-bit grayscale jpeg-images (Fig. 1A). We analyzed Fv/Fm and Y(II) along linear transects of duckweed fronds by means of the "plot profile" function of ImageJ v1.45 (Abràmoff et al., 2004) (Fig. 1B, C). Each transsect was taken along the longitudinal axis, starting from the proximal (basal) and finishing at the distal (apical) end of the fronds. Relative pixel intensities (0–255) with their corresponding position (pixel number) were exported and processed further in MS Excel 2016. As both Fv/Fm and Y(II) theoretically can have a value between 0 and 1, the relative pixel intensities were converted back to quantum yield by the following formula:

$$Fv/Fm \; or \; Y(II) = (1/256)*pixel \; intensity$$
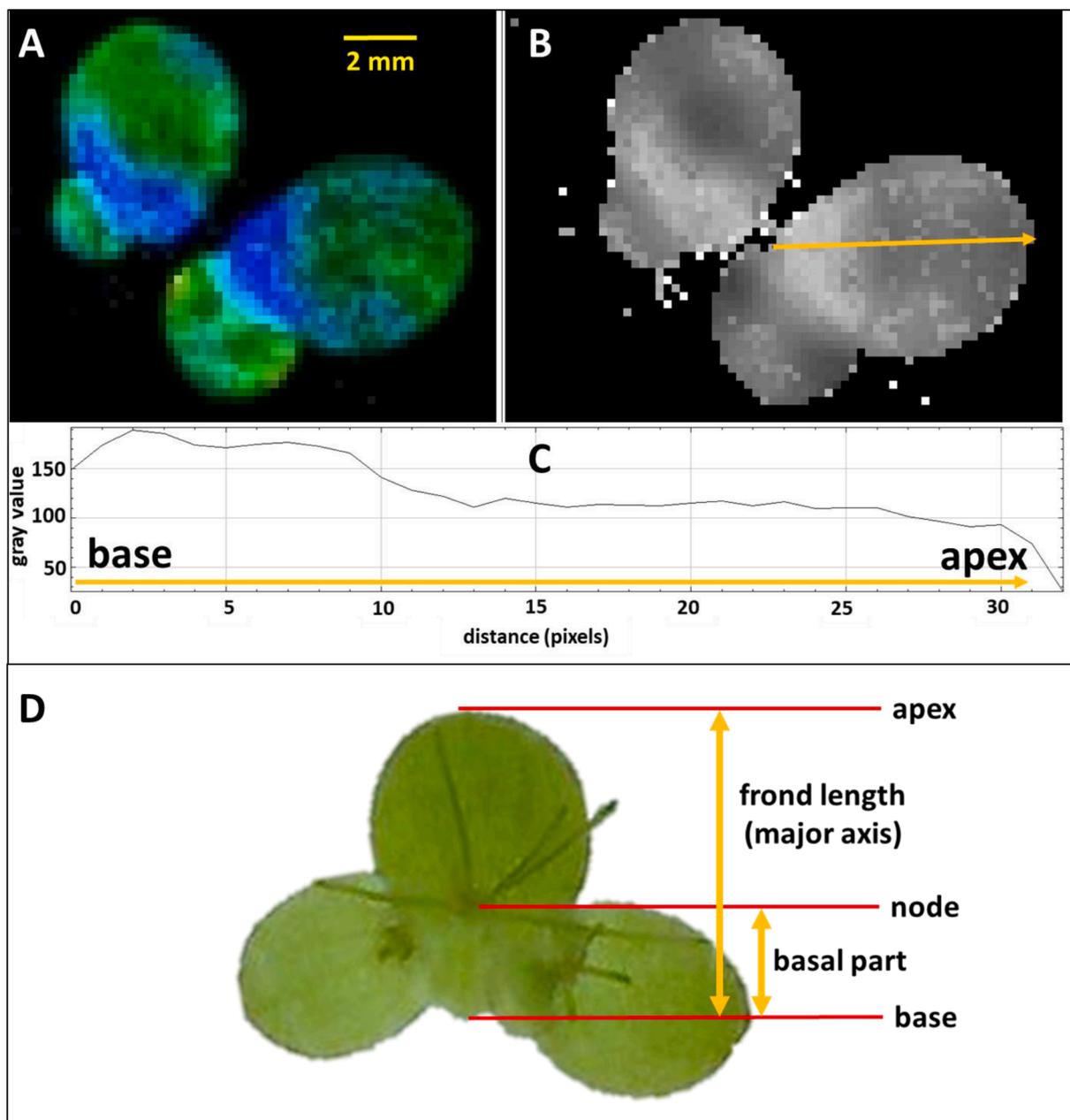
Fig. 1. Examples for analyses of chlorophyll fluorescence and scanned images, respectively: (A) False-color, and (B) grayscale Fv/Fm image of *S. polyrhiza* fronds treated with Ni for 72 h. The orange arrow in B indicates the linear transect along the longitudinal axis of a frond due to sample pixel values, C) profile of gray values along the sampled transect from B, corresponding to the Fv/Fm, D) scanned image of a control *La. punctata* colony, the orange arrows show the distance between the base and apex (i.e. frond length) and between the base and node (i.e. basal part) in a mother frond, respectively.

This way, the following data were derived for each frond of a culture:
-total frond length (=max pixel No * 0.22 mm),
-average Fv/Fm and Y(II) of each frond (=averaged pixel values along a transsect),
-relative position (=pixel No / max pixel No), Fv/Fm and Y(II) of each pixel along the longitudinal axis

In order to ensure sufficient spatial resolution, only fronds with a minimum of 12 pixels length (i.e. ~2.6 mm) were analyzed further.

The length of the basal part, that is the species-specific position of nodes in mature fronds was also determined. For this, we scanned the abaxial surface of 30–30 control colonies per species using a flatbed scanner (600 dpi, HP PSC 2175). These scanned images were analyzed by means of ImageJ v1.45 (Abràmoff et al., 2004). The relative distance from the frond basal end to the node was expressed as% of the total frond length measured along the longitudinal axis of mature fronds (Fig. 1D).

2.4. Data processing and statistical analyses

Pairwise comparisons between the data on heavy metal-treated and control plants were performed by means of two sample Mann-Whitney tests. Comparisons across different species were performed using the Kruskal-Wallis test and, in case of significant differences, by *post hoc* Mann-Whitney pairwise comparisons.

Descriptive statistics of morphometric and chlorophyll fluorescence data were performed by the "summary statistics" function of Past 4.0 (Hammer et al., 2001). The length distribution of the fronds measured in the chlorophyll fluorescence images was assessed by the "density" function of RStudio v1.1.463 (RStudio Team, 2020).

The assumed correlation of frond length with PSII quantum yields was tested by fitting linear ordinary least squares regression models and calculating Pearson's correlation. To compare heavy metal-induced responses as a function of frond size, the slopes of the regression models were compared by means of Past 4.0 (Hammer et al., 2001).

To analyze within-frond patterns of PSII quantum yields, each frond was classified into two categories based on its length, hereinafter referred to as young and mature, respectively. Fronds were considered as young if their size was below the median length of the respective control frond length, otherwise it was classified as mature. In both groups, pixel values at 5, 15, 25, 35, 45, 55, 65, 75, 85 and 95 % of the full transect length, measured from the proximal (basal) to the distal (apical) end, were used for within-frond heterogeneity analyses in Past 4.0 (Hammer et al., 2001). The assumed heterogeneity was tested by means of Kruskal-Wallis test, using data normalized to the means of their respective fronds. In case of significant result, the differences were compared pairwise by Bonferroni-corrected *post hoc* Mann-Whitney test.

5 % probability level, i.e., $p < 0.05$ was considered as the threshold for statistical significance in all analyses.

3. Results

3.1. Culture-level responses of duckweed species

Among the control cultures, *S. polyrhiza* displayed the slowest growth and formed the largest colonies (Table 1). *La. punctata* grew faster and formed the smallest colonies, while *Le. minor* had the highest RGR$_{FN}$ and an intermediate colony size (Table 1). Fv/Fm and Y(II) of control cultures showed a different order of species (Table 1): in general, control plants of *La. punctata* had the highest Fv/Fm and Y(II), while *S. polyrhiza* and *Le. minor* had similar Fv/Fm values, but the latter species displayed higher Y(II) than the former one. *La. punctata* had the lowest proportion of both regulated [Y(NPQ)] and non-regulated [Y(NO)] non-photochemical quenchings, though its Y(NPQ) did not differ significantly from that of *Le. minor*. *S. polyrhiza*, on the other hand, had the highest Y(NPQ), while its Y(NO) was similar to that of *Le. minor* (Table 1).

The heavy metals nickel and chromium caused a significant decrease in RGR$_{FN}$ of the tested species at the applied concentrations (Fig. 2A). In response to Cr(VI), the growth of the three metal-exposed species did not differ significantly. When exposed to nickel, *La. punctata* displayed a low sensitivity in terms of growth, while *S. polyrhiza* proved to be the most sensitive. Ni also triggered breaking-up of colonies, thus decreasing the mean colony size with the greatest extent for *S. polyrhiza* and a lowest one for *La. punctata* (Fig. 2B). Cr(VI) did not decrease significantly the colony size in either species, only *Le. minor* showed a slightly lowered value (Fig. 2B).

Fv/Fm values indicated a different sensitivity order of the tested species than RGR$_{FN}$ (Fig. 2C). Cr(VI)-treatments decreased Fv/Fm stronger in *Le. minor* than in the other two species. In Ni-treatments, Fv/Fm indicated that *S. polyrhiza* was most sensitive compared to *La. punctata* and *Le. minor*. Inhibition of Y(II) by Cr(VI) was similar in all three species, while Ni impacted Y(II) substantially in *S. polyrhiza*, but caused just a slight decrease in the other two species (Fig. 2D).

Both Y(NPQ) and Y(NO) of *S. polyrhiza* increased slightly in response to Cr(VI) treatments, but showed the strongest rise amongst the tested species due to Ni-treatments (Fig. 2E-F). Cr(VI)-treated *La. punctata* displayed strong up-regulation of Y(NPQ), and a slight increase in Y(NO). As a result of Ni treatments, this species showed an intermediate increase in Y(NPQ), but only a slight change in Y(NO) (Fig. 2E-F). The increase in Y(NPQ) of *Le. minor* was between the other two species due to Cr(VI)-treatment, but that of Y(NO) slightly exceeded those of *S. polyrhiza* and *La. punctata*. In case of Ni treatments, *Le. minor* showed similar increase in both Y(NPQ) and Y(NO), which ranked this species as less responsive for the former, and intermediately responsive in terms of the latter parameter, respectively (Fig. 2E-F).

Control cultures displayed a negatively skewed frond size distribution, indicating that the dominant frond size class (based on frond length) was that of mature fronds (Fig. 3). The size distribution was less assymetric -i.e. showed a higher proportion of smaller fronds- in fast-growing *Le. minor* compared to slower-growing *La. punctata* and especially *S. polyrhiza* (Table S1).

Heavy metal treatments resulted in changes of size distribution patterns in a species- and heavy metal-specific way (Fig. 3). In *S. polyrhiza*, both Cr(VI) and Ni exposure resulted in a shift towards the dominance of smaller fronds, resulting in a more symmetrical distribution. In *Le. minor*, Cr(VI) had a very similar effect, resulting in a less skewed length distribution (Table S1). However, in *Le. minor* cultures, nickel increased the dominance of larger fronds (Fig. 3). In *La. punctata*, both Ni and Cr(VI) had only minor effects on frond length distribution.

Table 1

Mean (±SE) growth rates (RGR$_{FN}$), colony sizes, maximum (Fv/Fm) and actual quantum yields of PSII (Y(II), regulated (Y(NPQ) and non-regulated non-photochemical quenchings (Y(NPO)) in the control cultures on the 3rd day of tests. Different lower cases indicate significant differences ($p < 0.05$) of species ($n = 12$–12 for *S. polyrhiza*, *La. punctata*, and $n = 8$ for *Le. minor*, respectively).

	RGR$_{FN}$ (day^{-1})	colony size (frond colony^{-1})	Fv/Fm (a.u.)	Y(II) (a.u.)	Y(NPQ) (a.u.)	Y(NO) (a.u.)
S. polyrhiza	0.251±0.010[c]	5.21±0.31[a]	0.748±0.001[b]	0.492±0.005[c]	0.224±0.003[a]	0.283±0.005[a]
La. punctata	0.306±0.012[b]	3.18±0.11[b]	0.781±0.001[a]	0.595±0.002[a]	0.156±0.002[b]	0.249±0.001[b]
Le. minor	0.375±0.010[a]	3.56±0.19[b]	0.749±0.001[b]	0.551±0.003[b]	0.163±0.004[b]	0.287±0.005[a]
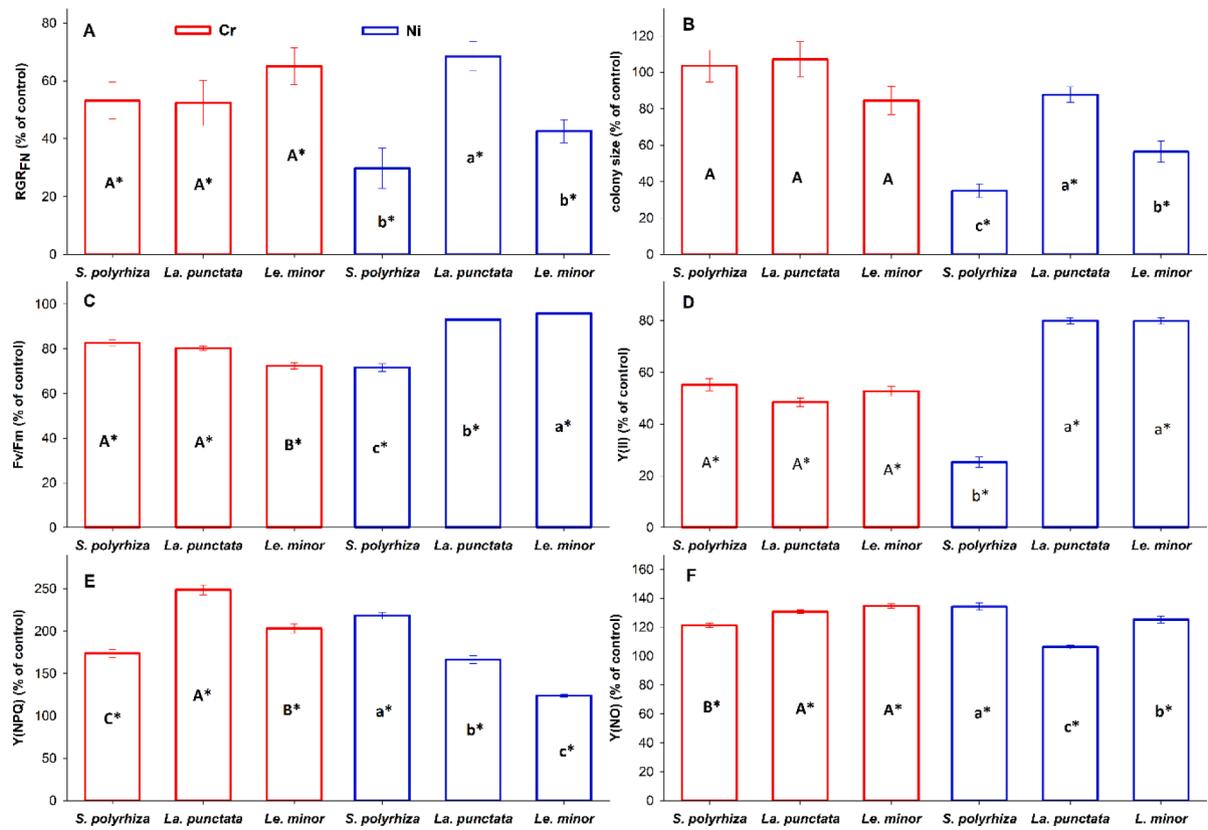
Fig. 2. The effects of 72 h-long treatments with 4 mg l^{-1} Cr(VI) (red bars, left) and 2.5 mg l^{-1} Ni (blue bars, right) as compared to the respective controls of each species on A: frond number-based relative growth rates (RGR$_{FN}$), B: average colony sizes, C: potential photochemical quantum yield (Fv/Fm), D: actual photo-chemical quantum yield (Y(II), E: regulated non-photochemical quenching (Y(NPQ), and F: non-regulated non-photochemical quenching (Y(NO). Means±SE of n = 12–12 for *S. polyrhiza, La. punctata*, and n = 8 for *Le. minor*, respectively. Different capitals for Cr(VI), and lower cases for Ni denote significant differences ($p < 0.05$) of species regarding the respective treatments. Asterisks indicate significant differenes ($p < 0.05$) compared to the respective control of the given species.
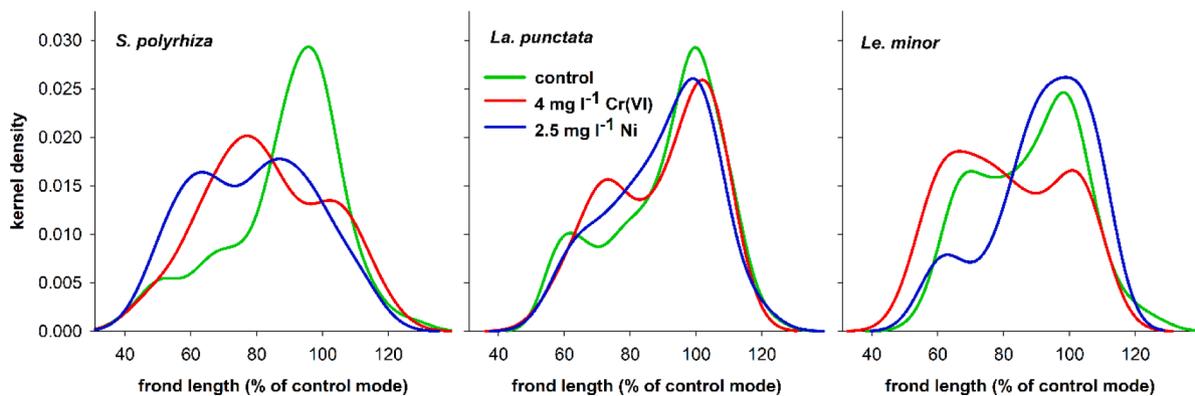

Fig. 3. Frond size distribution (as kernel density estimation) of the studied duckweed species growing in pure Steinberg's medium (control, green), 4 mg l^{-1} Cr(VI) (red), or 2.5 mg l^{-1} Ni (blue), respectively. Frond sizes were normalized to the respective species' control mode frond length (for summary statistics see Table S1).

3.2. Frond-level photosynthetic responses

Both Fv/Fm and Y(II) showed a strong positive correlation with frond length in control cultures of every species (Fig. 4., Table S2). The slope of this relationship, however, was small for both parameters within the studied frond size range. When treated with Cr(VI) or Ni, the three species showed a different response pattern of Fv/Fm as function of frond length (Fig. 4, Tables S2-S3). In Cr(VI)-treated *S. polyrhiza*, Fv/Fm of smaller (i.e. young) fronds had declined more compared to larger (i.e. mature) fronds. As a result, the slope of the regression model became steeper (Fig. 4A). The regression model for the Y(II) of Cr(VI)-

treated fronds, on the other hand, showed a slope similar to that of the control of the same species (Fig. 4B). Ni-treated *S. polyrhiza* fronds showed another pattern, with a greater decrease, i.e. higher Ni-sensitivity of the mature fronds (Fig. 4A, B).

In *La. punctata* plants (Fig. 4C-D), young fronds showed lower inhibition of PSII activity due to Cr(VI) exposure, but a higher inhibition when exposed to Ni, compared to the mature fronds. *Le. minor* plants exhibited similar responses to Ni- and Cr-treatments: both metals had a stronger impact on the young fronds compared to the mature ones (Fig. 4E-F). It should be noted, that for Cr(VI)-treated *Le. minor*, the correlation coefficient of Y(II) as a function of frond length was not
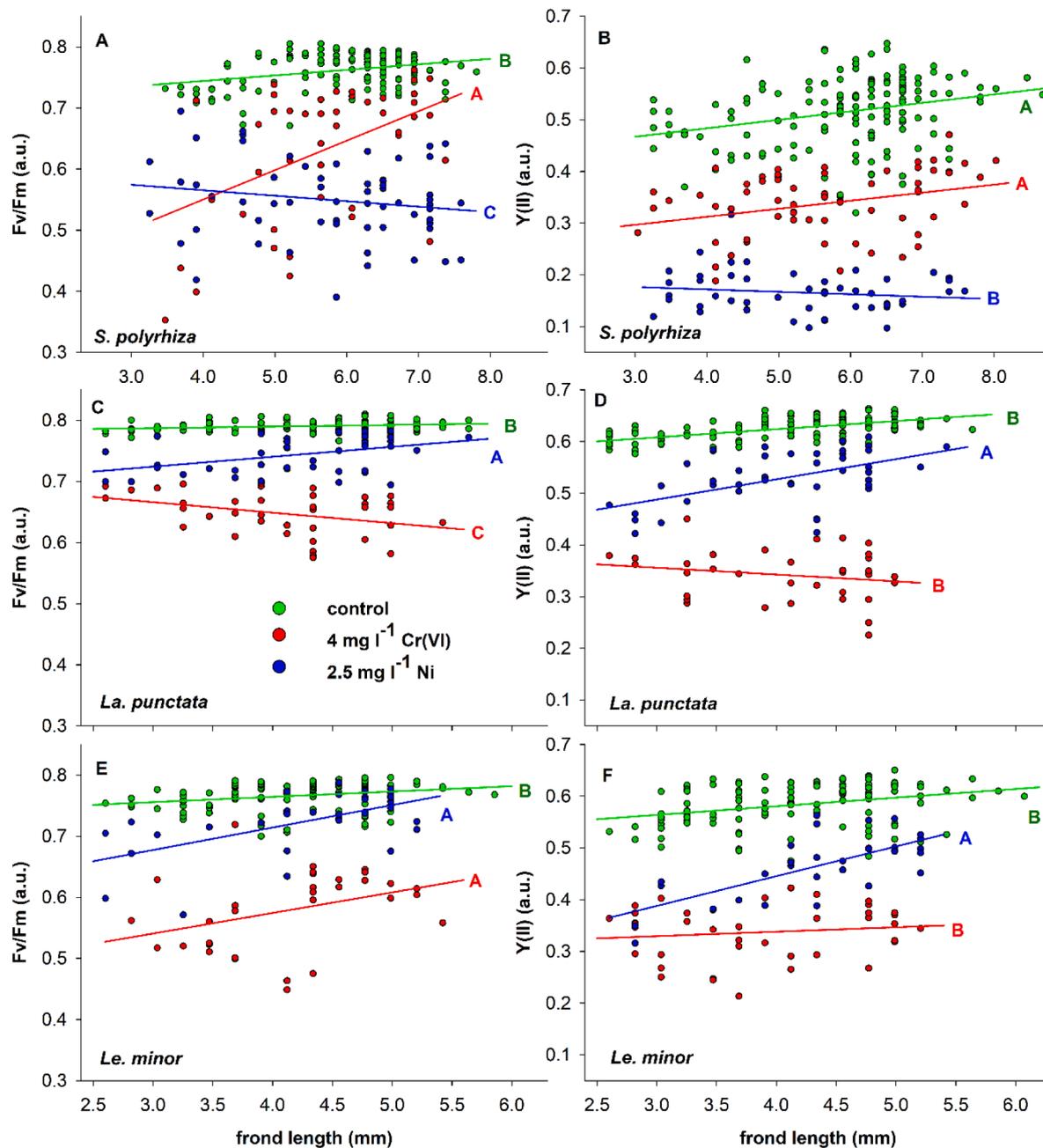
Fig. 4. Correlation between the frond length and the dark adapted photochemical efficiency (Fv/Fm, A, C, E) and actual photochemical quantum yield of PSII (Y(II), B, D, F) in duckweed cultures grown on either pure Steinberg's medium (control, green), 4 mg l^{-1} Cr(VI) (red), or 2.5 mg l^{-1} Ni (blue). Symbols denote individual fronds, lines with corresponding colors denote ordinary least squares linear regression models. Different capitals denote significantly ($p < 0.05$) different slopes of the regression models in case of the respective plot.

significant (Table S2), and the slopes did not differ significantly between this treatment and the control (Table S3). On the other hand, Ni-treated mature fronds displayed comparable Fv/Fm and Y(II) values similar to control fronds, while young Ni- treated fronds showed reduced photosynthetic quantum yields.

3.3. Within-frond photosynthetic patterns

In control cultures, we observed distinct within-frond longitudinal patterns of Fv/Fm as a function of species and frond maturity (Fig. 5). In general, young control fronds displayed an increasing trend in the photochemical efficiency from the base towards the apex, except of Fv/Fm in *La. punctata* (Fig. 5C). The basal part in mature control fronds was shortest in *S. polyrhiza* (25.5 ± 0.5 % of the total frond length), but

constituted more to the frond in *La. punctata* (34.4 ± 0.6 %) and *Le. minor* (33.0 ± 0.7 %). In all species, a definite Fv/Fm increase was found in these fronds from the basal end till the node (Fig. 5B,D,F). In *S. polyrhiza* and *La. punctata*, Fv/Fm stayed nearly constant or rose only slightly from the node up to the apex. In *Le. minor*, Fv/Fm decreased gradually from the fronds' middle region towards the apex (Fig. 5F).

Heavy metal treatments influenced the within-frond Fv/Fm patterns in a strongly metal- and age-dependent manner (Fig. 5). Cr(VI) primarily affected the peripheral frond regions in each species. Consequently, in young fronds Fv/Fm was the highest in the basal parts still attached to the pouch and showed a gradual decline towards the apex (Fig. 5A,C,E). In mature fronds, both basal and apical regions had lower Fv/Fm values than the middle parts (Fig. 5B,D,F). Ni-treatments resulted in a different spatial pattern of Fv/Fm as compared to Cr(VI). Ni had a stronger impact
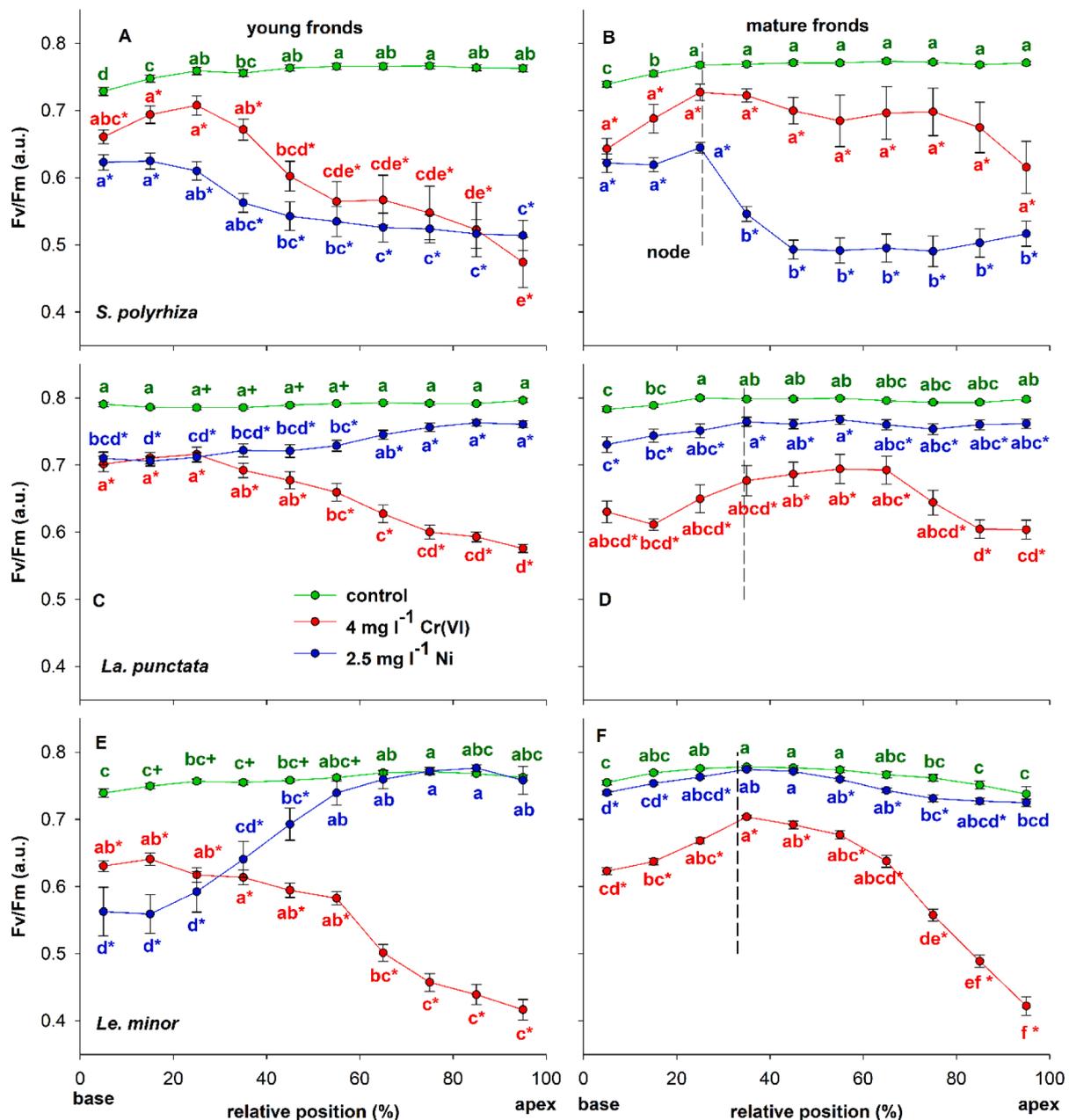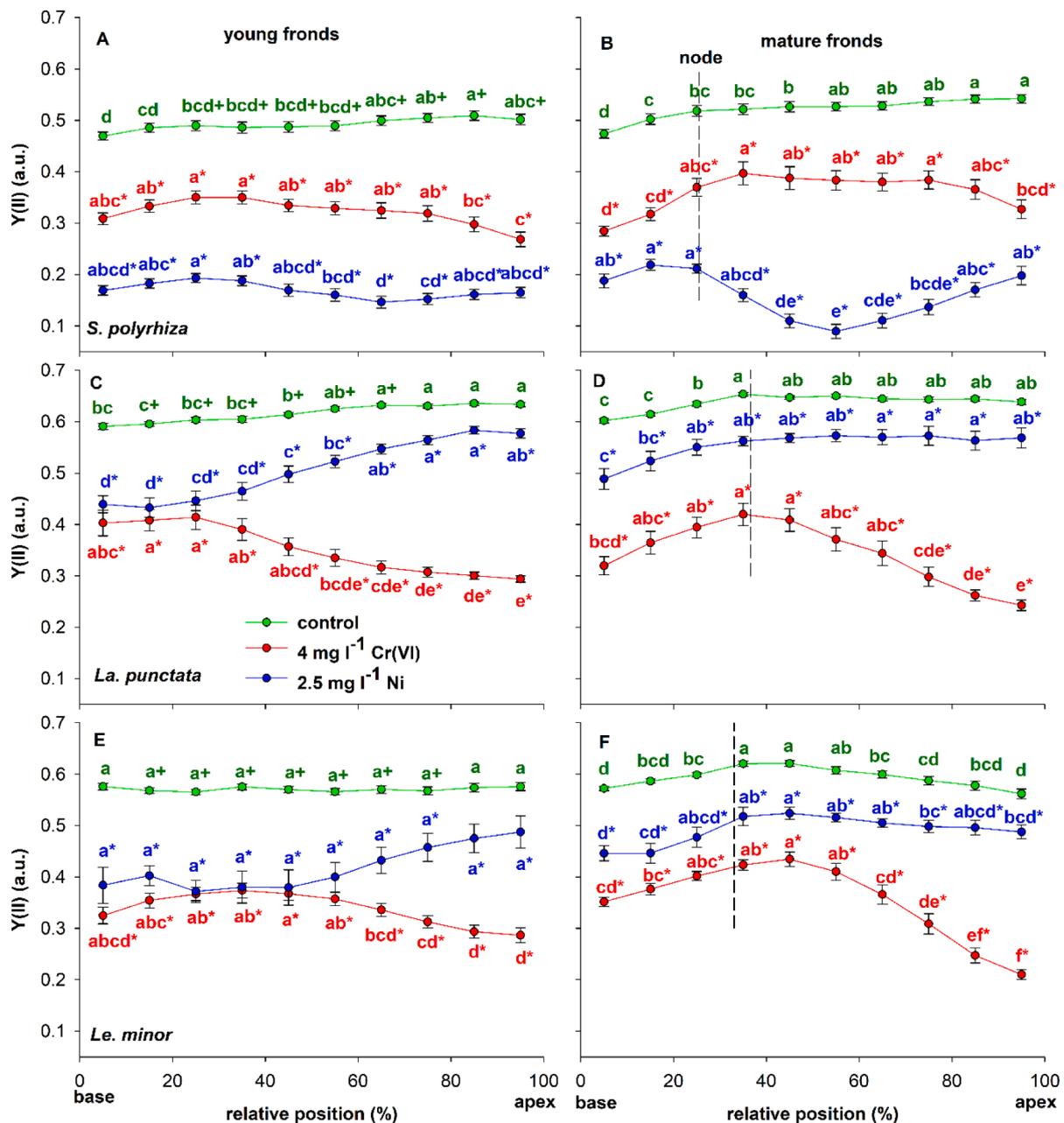
Fig. 5. Patterns (means±SE) in the dark adapted potential photochemical quantum yield of PSII (Fv/Fm) along the longitudinal axis of young (A, C, E) and mature (B, D, F) fronds grown in either pure Steinberg's medium (control, green), 4 mg l^{-1} Cr(VI) (red), or 2.5 mg l^{-1} Ni (blue), respectively. Different lower cases denote significant ($p < 0.05$) differences within the given frond transect. Asterisks indicate significant ($p < 0.05$) differences compared to the respective control at the given relative position. Crosses in case of young control fronds indicate significant ($p < 0.05$) differences compared to the respective control mature frond data at the given relative position. Dashed vertical lines for mature fronds (B, D, F) indicate the species-specific relative position of node along the fronds' axis.

on Fv/Fm in the basal regions of *La. punctata* and *Le. minor* young fronds (Fig. 5C,E) as compared to the apical parts. Indeed, the latter ones maintained similar Fv/Fm as the respective controls. In mature fronds of these two species, Ni-treatment affected less the within-frond patterns of Fv/Fm (Fig. 5D,F). However, *S. polyrhiza* responded differently to Ni: Fv/Fm was the highest at the basal regions of both the young and mature fronds and showed a gradual decline towards the apex (Fig. 5A, B). An almost general feature of Fv/Fm in all treatments and species was that positional trends changed around the morphometric position of the node. Though this kind of "turning point" was also typical to mature control fronds, the heavy metal treatments pronounced its presence even further, such as in case of Ni-treated *S. polyrhiza* (Fig. 5B) and Cr(VI)-treated *Le. minor* (Fig. 5F).

Spatial patterns of Y(II) in control fronds resembled those of Fv/Fm

when the respective species and maturity stages of fronds were compared (Fig. 6). Young control fronds of *Le. minor*, as an exeption, showed no basipetal trend in this parameter (Fig. 6E).

The Y(II) of heavy metal-treated fronds showed similar species-, position- and treatment-dependent patterns as Fv/Fm, but the within-frond gradients in Y(II) were in some cases more pronounced (Fig. 6). Differences in sensitivity of frond regions became more evident in *La. punctata* and *Le. minor*. Those parts which displayed almost the same Fv/Fm under Ni-treatments than control, i.e. mature fronds and maturing regions of young fronds, suffered stronger PSII inhibition under actinic light (Fig. 6C, E). Similarly, in mature fronds of *S. polyrhiza* a strong depression of Y(II) became apparent in the middle zone due to Ni treatments (Fig. 6B). In contrast, the basal segments in young fronds of *S. polyrhiza* showed similarly strong decline in PSII efficiency to that of

Fig. 6. Patterns (means±SE) in the actual photochemical efficiency (Y(II) along the longitudinal axis of young (A, C, E) and mature (B, D, F) fronds grown in either pure Steinberg's medium (control, green), 4 mg l^{-1} Cr(VI) (red), or 2.5 mg l^{-1} Ni (blue), respectively. Different lower cases denote significant ($p < 0.05$) differences within the given frond transect. Asterisks denote significant ($p < 0.05$) differences compared to the respective control at the given relative position of the transect. Crosses in case of young control fronds indicate significant ($p < 0.05$) differences compared to the respective control mature frond data at the given relative position. Dashed vertical lines in B, D and F indicate the species-specific relative position of node along the fronds' axis.

the maturing apical parts (Fig. 6A).

4. Discussion

4.1. Culture-level responses of the tested duckweed species

The heavy metal treatments strongly affected plant growth in a species- and metal-specific manner. Higher Ni-sensitivity of *S. polyrhiza* compared to *La. punctata* and *Le. minor* has previously been reported (Xyländer and Augsten, 1992; Appenroth et al., 2010), which may be due to the more efficient Ni-uptake by the former species under identical conditions (Oláh et al., 2023). Regarding Cr(VI) tolerance, Appenroth et al. (2008) found only negligible differences between *S. polyrhiza* and

Le. minor. These reports are consistent with our findings.

Frond length distributions showed that heavy metal treatments strongly affected not only frond production but also elongation of already formed fronds. Nickel is known to both inhibit cell division and restrict plant cell expansion (Yusuf et al., 2011; Hassan et al., 2019). Chromate may impair plant growth by disrupting cell division and interfering with assimilation, nutrient and water homeostasis (DalCorso, 2012; Ali et al., 2023). Disturbed frond development by heavy metals has previously been reported for various duckweed species (see e.g. Appenroth et al., 2003; Reale et al., 2016 for Cr(VI), and Xyländer et al., 1990; Appenroth et al., 2010 for Ni). Such a response can also be actively coordinated by a crosstalk between the cells' altered redox state (i.e. reactive oxygen species) and auxin distribution (Tognetti et al., 2012).

These so-called generic stress-induced morphogenic responses ("SIMRs", Potters et al., 2007) have already been linked to the effects of e.g. alumina nanoparticles on duckweeds (Juhel et al., 2011) and may have a role during acclimation to unfavorable conditions. In our study the three tested species showed divergent morphological responses. *S. polyrhiza* responded to the exposure to both heavy metals with an increased share of smaller fronds. This pattern points to arrested frond expansion throughout the maturation process. *Le. minor* responded similarly to Cr (VI). However, this species exhibited stronger dominance of larger fronds under Ni treatment which can be explained by the high sensitivity of forming fronds to this metal. In *La. punctata* as a contrast, the frond-length distributions remained relatively insensitive to treatments with either metal.

Metal-induced changes in the chlorophyll fluorescence parameters, however, showed a different sensitivity order of species than inhibition of growth. This discrepancy stresses the fact that growth- and chlorophyll fluorescence-derived phytotoxicity endpoints may be complementary, but not interchangeable (Oláh et al., 2021).

4.2. Frond-level responses

Data showed a gradual build-up in the assimilating capacity (Fv/Fm and Y(II)) along with frond ontogenesis. Higher photochemical efficiency of mature duckweed fronds, compared to their offspring was also reported by Lahive et al. (2012). At frond-level, the studied species exhibited different photosynthetic responses to the two applied heavy metals as a function of frond size. In *S. polyrhiza*, smaller fronds suffered higher PSII inhibition in response to Cr(VI), and lower inhibition to Ni, compared to mature fronds. In *La. punctata*, the opposite was observed, that is higher sensitivity of mature fronds to Cr(VI) and lower sensitivity to Ni as compared to the younger ones. In *Le. minor*, the younger fronds were more prone to both Cr(VI) and Ni-toxicity. Thus, the ontogenetic stage is an important determinant of plant metal stress in a metal-specific manner. The importance of ontogenetic stage in vulnerability of plant organs to heavy metals has been reported extensively for terrestrial plants (Krupa and Moniak, 1998; Riesen and Feller, 2005; DalCorso, 2012; Hassan et al., 2019). Age-related responses of duckweed fronds, however, have rarely been discussed so far. Lahive et al. (2012) found that Zn-treatments affected PSII function stronger in the younger fronds of *La. punctata*, *Le. minor* and *Le. gibba* than in the more mature ones. Our results for Ni-treated *La. punctata* and *Le. minor* confirmed that younger fronds were impacted stronger. This may relate to the observation that Ni is readily retranslocated within plants, i.e. from the older organs to the younger ones (Riesen and Feller, 2005). Analyses using µXRF have provided evidence of Ni retranslocation in the three duckweed species (Oláh et al., 2023). The opposite pattern, that is higher sensitivity of the older fronds compared to the younger ones in both Ni-treated *S. polyrhiza* and Cr(VI)-treated *La. punctata* can be related to heavy metal-induced senescence. A similar pattern was reported in Cd-treated *S. polyrhiza* mother fronds compared to their younger offspring (Peršić et al., 2022). The species- and concentration-specificity of this response type, however, is yet to be revealed.

All in all, these diverging patterns indicate that species- and ontogeny-dependent differences may modulate duckweeds' environmental responses to metals, and great care should be taken in generalizing duckweed stress responses from single measurements.

4.3. Within-frond patterns

In young fronds of control cultures, a basipetal increase in PSII efficiency was observed. Mature control fronds of *S. polyrhiza* and *La. punctata* displayed similar within-frond patterns. Photochemical efficiency increased gradually from the basal end towards the middle zone of the fronds, and then it stayed nearly constant up to the apical tip. In contrast, in *Le. minor*, the spatial pattern comprised of decreasing Fv/Fm and Y(II) values from the middle frond region towards the apex.

Ontogenetic differences within mature fronds may play lesser role in these observed basipetal patterns, but functional differences, e.g. the presence of meristems, may be hypothesized.

Different spatial zones of both young and mature fronds displayed different sensitivity to Ni and Cr(VI). In *La. punctata* and *Le. minor*, Ni predominantly inhibited PSII in young tissues, while mature fronds and frond segments were less affected. Ni easily migrates via the xylem and phloem and tends to accumulate in younger organs (Yusuf et al., 2011; Hassan et al., 2019). Thus, we hypothesize that a higher Ni uptake rate by offspring is a less likely cause of differential sensitivities than Ni re-translocation towards the younger tissues A similar mechanism may explain the reported accumulation of Cd in the node, veins and meristematic pocket compared to the main body of *La. punctata* fronds (Xu et al., 2018). Toxicity due to enhanced metal accumulation may be further accelerated by a higher sensitivity and/or a less efficient defense of developing tissues (Lahive et al., 2012). In *S. polyrhiza*, on the other hand, strong inhibition by Ni was found irrespective of frond age. This can be explained by higher Ni accumulation and/or generally higher sensitivity of this species to Ni as has previously been reported (Appenroth et al., 2010; Oláh et al., 2023).

Cr(VI) treatment yielded a more consistent within-frond pattern of photochemical efficiency among duckweed species. The primary targets of Cr(VI)-induced damage were the frond margins, especially the apical parts of both young and mature fronds. Terrestrial plants take Cr(VI) up by roots and transport it in the xylem to the aerial parts (Ali et al., 2023). In the leaves, Cr(VI) induces chlorosis and burning, especially in the margins and tips (Singh, 2001). Our previous µXRF analyses on the same three duckweed species also indicated an enhanced Cr accumulation in the frond peripheral regions and veins (Oláh et al., 2023). The analogous Cr accumulation patterns in aquatic and terrestrial plants suggest that internal translocation may play a dominant role, rather than different rates of metal uptake in different parts of fronds.

The basipetal trends in photochemical efficiency clearly changed in the vicinity of the node both in control and heavy metal-treated fronds. This suggests functionally distinct parts of fronds, separated by a physiological barrier marked by the node. Meristematic pouches are localized in the basal part of fronds, delineated by the node (Landolt, 1986). Since offspring is produced in this region, its assimilating capacity may be lower, but the rest of the frond can easily compensate for this trade-off. In protecting this region, veins may play an important role in directing potential toxins away. Veins can disperse toxic substances towards the central and apical frond parts that have no crucial role in producing offspring. From this perspective, colony disintegration and dropping-off roots by fronds can also be considered as preventive mechanisms that cut-off internal transport of toxicants. Amongst other factors, enhanced frond abscission was reported in response to heavy metals (Henke et al., 2011). Li and Xiong (2004) found forced frond abscission due to Cd in *Lemna paucicostata* (current name is *Lemna aequinoctialis*), and hypothesized that it can prevent metal translocation towards the daughter fronds. In this study, Ni caused significant colony breakup at the applied concentration, but not Cr(VI). An explanation for that can be that the latter metal is primarily translocated to, and accumulated at, the distal parts of the fronds.

This study represents only a small subset of the 36 duckweed species, and used only one concentrations of two heavy metals. Furthermore, this study focused only on rapid internal metal distribution responses (<72 h). It is likely that long term responses to metals are even more complex due to the additional induction of phenotypic alterations. Nevertheless, the obtained results point to contrasting species-, age- and substance-specific plant responses. These findings highlight the, so far, underexplored potential of frond- and within-frond level analyses in these tiny plants. Future research with such recently emerging techniques as single-cell sequencing (Abramson et al., 2022), or joint imaging approaches, promises to further resolve the functional differentiation in duckweed fronds and colonies.

5. Conclusions

Our results demonstrate that duckweed colonies and fronds consist of functionally different parts that show distinct responses to environmental stimuli. Such differences are masked when one analyzes averaged responses of a duckweed culture in routine tests. Duckweed species are widely utilized in plant physiology and ecotoxicology research, and also have an increasing economic significance. All those applications rely strongly on the interactions between the duckweed colony and its environment. Therefore, detailed frond-level analysis of duckweed responses by various imaging methods offers a unique asset to gain better insight into the functioning of these widely used model organisms. Since many of those imaging techniques use *in vivo*, non-invasive approaches, such methods bear the promise to facilitate repeated, time-resolved analyses, or joint measurements of multiple aspects of duckweed environmental responses on the same colonies.

CRediT authorship contribution statement

Viktor Oláh: Conceptualization, Methodology, Formal analysis, Writing – original draft, Visualization, Funding acquisition. **Kamilla Kosztankó:** Investigation. **Muhammad Irfan:** Investigation. **Zsuzsanna Barnáné Szabó:** Investigation. **Marcel A. K Jansen:** Writing – review & editing. **Sándor Szabó:** Writing – review & editing. **Ilona Mészáros:** Writing – review & editing.

Declaration of competing interest

The authors declare that they have no known competing financial interests or personal relationships that could have appeared to influence the work reported in this paper.

Data availability

Data will be made available on request.

Supplementary materials

Supplementary material associated with this article can be found, in the online version, at doi:10.1016/j.stress.2024.100405.

References

Abràmoff, M.D., Magalhães, P.J., Ram, S.J., 2004. Image processing with ImageJ. Biophotonics Int. 11, 32–64.

Abramson, B.W., Novotny, M., Hartwick, N.T., Colt, K., Aevermann, B.D., Scheuermann, R.H., Michael, T.P., 2022. The genome and preliminary single-nuclei transcriptome of *Lemna minuta* reveals mechanisms of invasiveness. Plant Physiol. 188, 879–897. https://doi.org/10.1093/plphys/kiab564.

Acosta, K., Appenroth, K.J., Borisjuk, L., Edelman, M., Heinig, U., Jansen, M.A.K., Oyama, T., Pasaribu, B., Schubert, I., Sorrels, S., Sree, K.S., Xu, S., Michael, T.P., Lam, E., 2021. Return of the *Lemnaceae*: duckweed as a model plant system in the genomics and postgenomics era. Plant Cell 33, 3207–3234. https://doi.org/10.1093/plcell/koab189.

Ali, S., Mir, R.A., Tyagi, A., Manzar, N., Kashyap, A.S., Mushtaq, M., Raina, A., Park, S., Sharma, S., Mir, Z.A., Lone, S.A., Bhat, A.A., Baba, U., Mahmoudi, H., Bae, H., 2023. Chromium toxicity in plants: signaling, mitigation, and future perspectives. Plants 12, 1502. https://doi.org/10.3390/plants12071502.

Appenroth, K.J., Keresztes, Á., Sárvári, É., Jaglarz, A., Fischer, W., 2003. Multiple effects of chromate on *Spirodela polyrhiza*: electron microscopy and biochemical investigations. Plant Biol. 5, 315–323. https://doi.org/10.1055/s-2003-40801.

Appenroth, K.J., Luther, A., Jetschke, G., Gabrys, H., 2008. Modification of chromate toxicity by sulphate in duckweeds (*Lemnaceae*). Aquat. Toxicol. 89, 167–171. https://doi.org/10.1016/j.aquatox.2008.06.012.

Appenroth, K.J., Krech, K., Keresztes, Á., Fischer, W., Koloczek, H., 2010. Effects of nickel on the chloroplasts of the duckweeds *Spirodela polyrhiza* and *Lemna minor* and their possible use in biomonitoring and phytoremediation. Chemosphere 78, 216–223. https://doi.org/10.1016/j.chemosphere.2009.11.007.

Cedergreen, N., Madsen, T.V., 2002. Nitrogen uptake by the floating macrophyte *Lemna minor*. New Phytol. 155, 285–292. https://doi.org/10.1046/j.1469-8137.2002.00463.x.

DalCorso, G., Furini, A., 2012. Heavy metal toxicity in plants. Plants and Heavy Metals, SpringerBriefs in Molecular Science. Springer, the Netherlands, Dordrecht, pp. 1–25. https://doi.org/10.1007/978-94-007-4441-7_1.

Demmig-Adams, B., López-Pozo, M., Polutchko, S.K., Fourounjian, P., Stewart, J.J., Zenir, M.C., Adams, W.W., 2022. Growth and nutritional quality of *Lemnaceae* viewed comparatively in an ecological and evolutionary context. Plants 11, 145. https://doi.org/10.3390/plants11020145.

Environment Canada, 2007. Biological test method - Test for measuring the inhibition of growth using the freshwater macrophyte *Lemna minor*. In: Environmental Protection Service, Report EPS 1/RM/37, 2nd ed. Method Development and Applications Section, Environmental Technology Centre, Environment Canada, Ottawa, Canada, p. 112. ISBN 0-662-43340-8.

Hammer, Ø., Harper, D.A.T., Ryan, P.D., 2001. PAST: paleontological statistics software package for education and data analysis. Palaeontol. Electron 4, 9.

Hassan, M.U., Chattha, M.U., Khan, I., Chattha, M.B., Aamer, M., Nawaz, M., Ali, A., Khan, M.A.U., Khan, T.A., 2019. Nickel toxicity in plants: reasons, toxic effects, tolerance mechanisms, and remediation possibilities—A review. Environ. Sci. Pollut. Res. 26, 12673–12688. https://doi.org/10.1007/s11356-019-04892-x.

Henke, R., Eberius, M., Appenroth, K.J., 2011. Induction of frond abscission by metals and other toxic compounds in *Lemna minor*. Aquat. Toxicol. 101, 261–265. https://doi.org/10.1016/j.aquatox.2010.10.007.

Juhel, G., Batisse, E., Hugues, Q., Daly, D., van Pelt, F.N.A.M., O'Halloran, J., Jansen, M.A.K., 2011. Alumina nanoparticles enhance growth of *Lemna minor*. Aquat. Toxicol. 105, 328–336. https://doi.org/10.1016/j.aquatox.2011.06.019.

Klughammer, C., Schreiber, U., 2008. Complementary PS II quantum yields calculated from simple fluorescence parameters measured by PAM fluorometry and the saturation pulse method. PAM Application Notes 1, 27–35. https://www.walz.com/products/chl_p700/pan/overview-journals.html.

Krupa, Z., Moniak, M., 1998. The stage of leaf maturity implicates the response of the photosynthetic apparatus to cadmium toxicity. Plant Sci. 138, 149–156. https://doi.org/10.1016/S0168-9452(98)00159-9.

Lahive, E., O'Halloran, J., Jansen, M.A.K., 2012. Frond development gradients are a determinant of the impact of zinc on photosynthesis in three species of *Lemnaceae*. Aquat. Bot. 101, 55–63. https://doi.org/10.1016/j.aquabot.2012.04.003.

Landolt, E., 1986. The family of "*Lemnaceae*": a monographic study - Biosystematic investigations in the family of duckweeds ('*Lemnaceae*'). Geobotanisches Institut der ETH. Zürich, Switzerland.

Lemon, G.D., Posluszny, U., 2000. Comparative shoot development and evolution in the *Lemnaceae*. Int. J. Plant Sci. 161, 733–748. https://doi.org/10.1086/314298.

Li, T.Y., Xiong, Z.T., 2004. Cadmium-induced colony disintegration of duckweed (*Lemna paucicostata* Hegelm.) and as biomarker of phytotoxicity. Ecotoxicol. Environ. Saf. 59, 174–179. https://doi.org/10.1016/j.ecoenv.2003.11.007.

OECD, 2006. Guidelines the Testing of chemicals, Revised Proposal For a New For Guideline 221, *Lemna* sp. Growth Inhibition Test.

Oláh, V., Lakatos, G., Bertók, C., Kanalas, P., Szőllősi, E., Kis, J., Mészáros, I., 2010. Short-term chromium(VI) stress induces different photosynthetic responses in two duckweed species, *Lemna gibba* L. and *Lemna minor* L. Photosynthetica 48, 513–520. https://doi.org/10.1007/s11099-010-0068-6.

Oláh, V., Hepp, A., Gaibor Vaca, N.Y., Tamás, M., Mészáros, I., 2018. Retrospective analyses of archive phytotoxicity test data can help in assessing internal dynamics and stability of growth in laboratory duckweed cultures. Aquat. Toxicol. 201, 40–46. https://doi.org/10.1016/j.aquatox.2018.05.022.

Oláh, V., Hepp, A., Irfan, M., Mészáros, I., 2021. Chlorophyll fluorescence imaging-based duckweed phenotyping to assess acute phytotoxic effects. Plants 10, 2763. https://doi.org/10.3390/plants10122763.

Oláh, V., Irfan, M., Szabó, Z.B., Sajtos, Z., Ragyák, Á.Z., Döncző, B., Jansen, M.A.K., Szabó, S., Mészáros, I., 2023. Species- and metal-specific responses of the ionome of three duckweed species under chromate and nickel treatments. Plants 12, 180. https://doi.org/10.3390/plants12010180.

Paolacci, S., Stejskal, V., Toner, D., Jansen, M.A.K., 2022. Wastewater valorisation in an integrated multitrophic aquaculture system; assessing nutrient removal and biomass production by duckweed species. Environ. Pollut. 302, 119059 https://doi.org/10.1016/j.envpol.2022.119059.

Park, J., Lee, H., Han, T., 2020. Comparative paraquat sensitivity of newly germinated and mature fronds of the aquatic macrophyte *Spirodela polyrhiza*. Am. J. Plant Sci. 11, 1008–1024. https://doi.org/10.4236/ajps.2020.117072.

Peršić, V., Antunović Dunić, J., Domjan, L., Zellnig, G., Cesar, V., 2022. Time course of age-linked changes in photosynthetic efficiency of *Spirodela polyrhiza* exposed to cadmium. Front. Plant Sci. 13, 872793 https://doi.org/10.3389/fpls.2022.872793.

Petersen, F., Demann, J., Restemeyer, D., Olfs, H.W., Westendarp, H., Appenroth, K.J., Ulbrich, A., 2022. Influence of light intensity and spectrum on duckweed growth and proteins in a small-scale, re-circulating indoor vertical farm. Plants 11, 1010. https://doi.org/10.3390/plants11081010.

Pietrini, F., Passatore, L., Fischetti, E., Carloni, S., Ferrario, C., Polesello, S., Zacchini, M., 2019. Evaluation of morpho-physiological traits and contaminant accumulation ability in *Lemna minor* L. treated with increasing perfluorooctanoic acid (PFOA) concentrations under laboratory conditions. Sci. Total Environ. 695, 133828 https://doi.org/10.1016/j.scitotenv.2019.133828.

Potters, G., Pasternak, T.P., Guisez, Y., Palme, K.J., Jansen, M.A.K., 2007. Stress-induced morphogenic responses: growing out of trouble? Trends Plant Sci. 12, 98–105. https://doi.org/10.1016/j.tplants.2007.01.004.

Reale, L., Ferranti, F., Mantilacci, S., Corboli, M., Aversa, S., Landucci, F., Baldisserotto, C., Ferroni, L., Pancaldi, S., Venanzoni, R., 2016. Cyto-histological and morpho-physiological responses of common duckweed (*Lemna minor* L.) to chromium. Chemosphere 145, 98–105. https://doi.org/10.1016/j.chemosphere.2015.11.047.

Riesen, O., Feller, U., 2005. Redistribution of nickel, cobalt, manganese, zinc, and cadmium via the phloem in young and maturing wheat. J. Plant Nutr. 28, 421–430. https://doi.org/10.1081/PLN-200049153.

Roháček, K., 2002. Chlorophyll fluorescence parameters: the definitions, photosynthetic meaning, and mutual relationships. Photosynthetica 40, 13–29. https://doi.org/10.1023/A:1020125719386.

RStudio Team, 2020. RStudio: integrated development for R. RStudio, PBC, Boston, MA. URL http://www.rstudio.com/.

Singh, A.K., 2001. Effect of trivalent and hexavalent chromium on spinach (*Spinacea oleracea* L). Environ. Ecol. 19, 807–810.

Szabó, S., Zavanyi, G., Koleszár, G., Del Castillo, D., Oláh, V., Braun, M., 2023. Phytoremediation, recovery and toxic effects of ionic gadolinium using the free-floating plant *Lemna gibba*. J. Hazard. Mater. 458, 131930 https://doi.org/10.1016/j.jhazmat.2023.131930.

Tippery, N.P., Les, D.H., Appenroth, K.J., Sree, K.S., Crawford, D.J., Bog, M., 2021. *Lemnaceae* and *Orontiaceae* are phylogenetically and morphologically distinct from Araceae. Plants 10, 2639. https://doi.org/10.3390/plants10122639.

Tognetti, V.B., Mühlenbock, P., Van Breusegem, F., 2012. Stress homeostasis – the redox and auxin perspective. Plant Cell Environ. 35, 321–333. https://doi.org/10.1111/j.1365-3040.2011.02324.x.

Ware, A., Jones, D.H., Flis, P., Chrysanthou, E., Smith, K.E., Kümpers, B.M.C., Yant, L., Atkinson, J.A., Wells, D.M., Bhosale, R., Bishopp, A., 2023. Loss of ancestral function in duckweed roots is accompanied by progressive anatomical reduction and a re-distribution of nutrient transporters. Curr. Biol. 33, 1795–1802. https://doi.org/10.1016/j.cub.2023.03.025 e4.

Xu, H., Yu, C., Xia, X., Li, M., Li, H., Wang, Y., Wang, S., Wang, C., Ma, Y., Zhou, G., 2018. Comparative transcriptome analysis of duckweed (*Landoltia punctata*) in response to cadmium provides insights into molecular mechanisms underlying hyperaccumulation. Chemosphere 190, 154–165. https://doi.org/10.1016/j.chemosphere.2017.09.146.

Xyländer, M., Augsten, H., 1992. Different sensitivity of some *Lemnaceae* to nickel. Beitr. Biol. Pflanz. 67, 89–99.

Xyländer, M., Liebert, H.P., Augsten, H., 1990. The influence of nickel on growth and nitrate reductase activity in *Lemnaceae*. Beitr. Biol. Pflanz. 65, 419–428.

Yusuf, M., Fariduddin, Q., Hayat, S., Ahmad, A., 2011. Nickel: an overview of uptake, essentiality and toxicity in plants. Bull. Environ. Contam. Toxicol. 86, 1–17. https://doi.org/10.1007/s00128-010-0171-1.